AUTONOMOUS LANDING OF A NOVEL MORPHING QUADROTOR WITH GROUND EFFECT

Zhen WANG[1], Xiao LIANG[2*],Yiwei XIU[3],Guodong CHEN[4]

Quadrotor is an unmanned aerial vehicle capable of vertical take-off and landing. Its small size makes it widely used in various fields. In order to further increase its flexibility, this paper proposes a morphing quadrotor that can be transformed into a four-wheeler when landing. First, the structure and mode transition process of the morphing quadrotor are introduced. Then, the dynamic model of the morphing quadrotor was established based on the conventional quadrotor model. Since the morphing quadrotor has obvious force changes when it is deformed near the ground, the mode transition process is decomposed and analyzed by the numerical calculation of flow field. Furthermore, the ground effect model of the transition process is established, which also improves the model of morphing quadrotor. Based on the model of the morphing quadrotor, the Proportional Integral Derivative (PID) and Linear Quadratic Regulator (LQR) controller are designed and compared with each other. The simulation results show that in the case of limited control input, the additional compensation of the lift is required to make the deformation process stable. It is recommended to add the lift compensation to achieve a smooth transition.

Keywords: Morphing Quadrotor, Autonomous Landing, Mode Transition, Ground Effect, Numerical Calculation of Flow Field

1. Introduction

Unmanned Aerial Vehicle (UAV) is increasingly used in complex environments for a variety of purposes, such as search, rescue, mapping, and exploring [1-3]. Quadrotor is a type of UAV with small size and lightweight, and it plays an important role in military and civilian fields, thus attracting the attention of many researchers [4]. In order to expand the flexibility of quadrotor, future quadrotor needs more advanced capabilities such as the ability to deform.

Morphing aircraft usually have multiple flight modes or states, and can complete many tasks that conventional aircraft cannot, such as avoiding obstacles by changing their shape [5], adjusting the angle of propeller inclination to achieve

[1] SN Eng., Beijing Institute of Space Mechanics & Electricity, China, e-mail: china_wangzhen@126.com
[2]* Prof., School of Automation, Shenyang Aerospace University, China, e-mail: connyzone@126.com (corresponding author)
[3] Eng., School of Automation, Shenyang Aerospace University, China, e-mail: anatsicc@163.com
[4] Eng., School of Astronautics, Harbin Institute of Technology, China, e-mail: cgd1128@163.com

faster speed [6]. However, it also brings great challenges to control system design. Many researchers have proposed a variety of control methods for different types of morphing aircraft. Desbiez et al. proposed a morphing quadrotor called X-Morf [7], which can actively change its geometric shape by adjusting the angle between rotor arms to fly thorough narrow gaps. Model reference adaptive control algorithm (MRAC) is designed to overcome the uncertainty of inertia and center of mass when the quadrotor deforms. But X-Morph can only achieve semi-autonomous deformation for the time being. By the control of Linear Quadratic Integral (LQI) and Proportional Integral Derivative (PID), Zhao M et al. [8] proposed a quadrotor that can carry objects by using deformable rotor, which does not need additional mechanical arms. The research is extended to three-dimensional folding deformation [9], but their mechanical joints are considered to be slowly deformed and the transition process is time-consuming.

In addition, some researchers combine the advantages of air and ground and propose the concept of amphibious aircraft, such as the unmanned aerial vehicle that can autonomously land on walls and telephone poles [10-11]. Keennon M et al. proposed a miniature aircraft (MAV) [12], which can realize the transition from the flight state to the walking state through telescopic wings. Yet, due to its fixed-wing structure, it is impossible to hover in the air. Obviously, there are still many challenges in amphibious morphing aircraft [13]. In this paper, a morphing quadrotor that has both flight mode as conventional quadrotor and ground mode as four-wheeler is studied. The dynamic model of this quadrotor will change greatly during mode transition process, so how to ensure the smoothness of the transition process is the subject of this paper.

The lift of most morphing quadrotors comes from their rotors. So similar to helicopters, ground effects will have a great impact on its take-off and landing. The conventional studies of quadrotor usually ignore ground effect or take it as interference which does not have model. So some anti-interference control methods such as robust control [14], backstepping control [15], neural network control [16], model reference adaptive control [17], H∞ control [18] and PID control [19] are proposed to eliminate the influence of ground effect. In recent years, the impact of ground effect on control system has gradually attracted the attention of researchers. In the outwash experiment of National Aeronautics and Space Administration (NASA) [20], the aircraft is placed in the environment with continuous ground effect interference. Through the hovering control of different heights, the data of ground effect is got and refined. Zorana et al. [21] carried out numerical analysis of flow field through the Unsteady Reynolds Average Navistokes (URANS) equation, and correctly estimated the performance of rotor under ground effect. By the experimental data of hovering control, Benjamin et al. [22] studied a flow solver named FLOWer and it can be used to calculate the distribution of flow field under the influence of ground effect.

In this paper, a novel morphing quadrotor that has both flight mode as conventional quadrotor and ground mode as four-wheeler is proposed. Then, the ground effect is analyzed and will be taken as a part of lift. Furthermore, the dynamic model of the morphing quadrotor is established, and the controller based on PID and Linear Quadratic Regulator (LQR) is designed and compared, respectively. The simulation results show that if the speed of rotors is not limited, both two control methods can realize the autonomous landing and deformation of morphing quadrotor. But LQR has a better performance on rapidity and overshoot and its mode transition process is smoother. If the speed of rotors is limited, it is recommended to add the lift compensation to keep the deformation stable.

2. Morphing Quadrotor with Flight Mode and Ground Mode

In order to further improve the flexibility and adaptability of quadrotor, the morphing quadrotor in this paper is shown in Fig. 1. It has both flight mode as conventional quadrotor and ground mode as four-wheeler. During landing, the mode changes from conventional quadrotor to four-wheeler and the four rotors can be transformed from 0° to 45°. This morphing quadrotor has the advantages of quadrotor and four-wheeler, so different states of mode will make it better adapt to different environments and save energy.

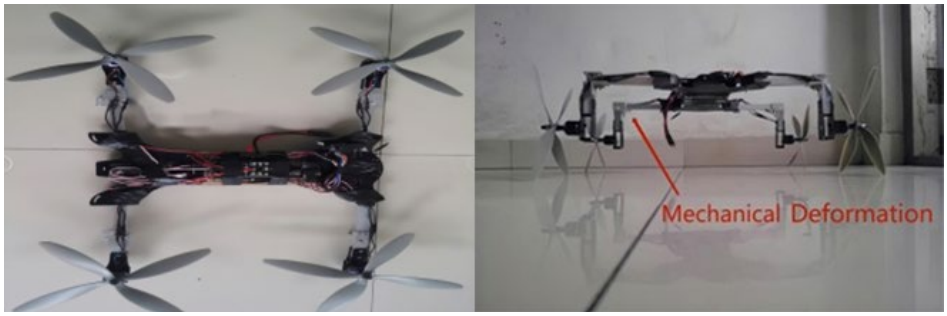

Fig. 1. The morphing quadrotor

The morphing quadrotor adopts an H-shaped body, and the control unit combined with four-way wireless remote control and four-way motor drive is responsible for sending and receiving signals to control the deformation of rotor arms; The reduction gear motor, trapezoidal screw, connecting rod mechanism and hinge constitute mechanical units, which pushes and pulls the four rotor arms to complete the mode transition process.

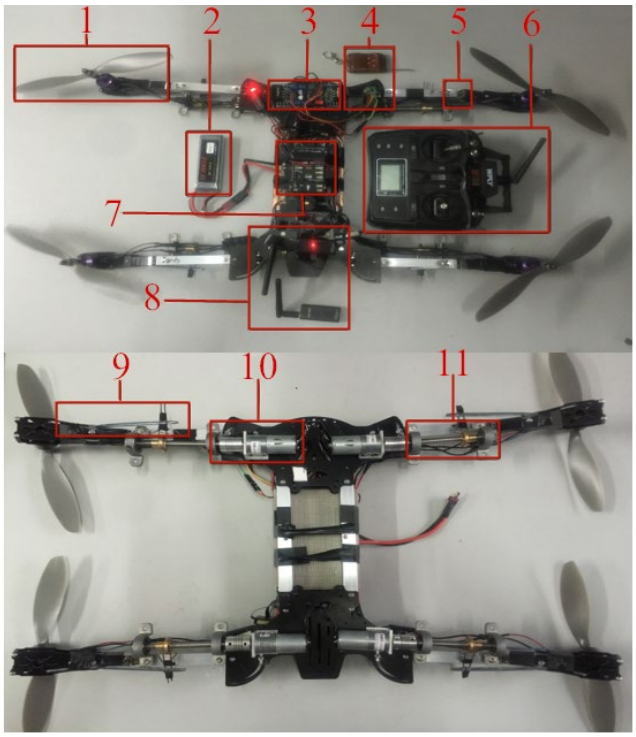

Fig. 2. Overall design of the H-type morphing quadrotor

As shown in Fig. 2: 1 is motor and propeller; 2 is lithium battery; 3 is motor drive; 4 is four-way wireless remote control; 5 is hinge structure; 6 is remote controller; 7 is flight control board; 8 is digital transmission station; 9 is connecting rod mechanism; 10 is reduction gear motor; 11 is trapezoidal screw.

3. Dynamic Model of Morphing Quadrotor

3.1 Dynamic Model of Conventional Quadrotor

Based on the analysis of the conventional quadrotor [23], the main forces and torques include: gravity, air resistance, rotational resistance moment, lift generated by rotors, gyro torque and axial torque when attitude changes.

According to Newton-Euler equation, the dynamic model of the conventional quadrotor is:

$$\begin{cases} \vec{F} = m\dfrac{d\vec{V}}{dt} = m\vec{a} = \vec{F}_f + \vec{F}_d + \vec{F}_g \\ \vec{M} = \dfrac{d\vec{H}}{dt} = \vec{I}\vec{\varepsilon} + \vec{\omega} \times \vec{I}\vec{\omega} = \vec{M}_\tau + \vec{M}_f - \vec{M}_d + \vec{M}_c \end{cases}. \tag{1}$$

In Eq. (1), $\vec{F}$ is the lift. $\vec{V}$ is the velocity relative to the ground coordinate system. m is the mass. $\vec{M}$ is the total torque relative to the body center of mass. $\vec{H}$, ω and $\vec{\varepsilon}$ are the angular momentum, the angular velocity and the angular acceleration respectively relative to the ground coordinate system.

Suppose that the control input of quadrotor is $u = [u_1, u_2, u_3, u_4]^T$, where u_1 represents the resultant force of the lift that controls altitude; u_2 represents the moment of the roll control; u_3 represents the moment of the pitch control; u_4 represents the moment of the yaw control. That is, the control input u is:

$$\begin{cases} u_1 = b({\omega_1}^2 + {\omega_2}^2 + {\omega_3}^2 + {\omega_4}^2) \\ u_2 = lb({\omega_4}^2 - {\omega_2}^2)/I_x \\ u_3 = lb({\omega_3}^2 - {\omega_1}^2)/I_y \\ u_4 = kb({\omega_1}^2 + {\omega_3}^2 - {\omega_2}^2 - {\omega_4}^2)/I_z \end{cases} . \tag{2}$$

In Eq. (2), b is the lift coefficient; l is the distance from the body center of the mass to the motor center of the mass; k is the air resistance coefficient; I_x is the rotational inertia around the x axis; I_y is the rotational inertia around the y axis; I_z is the rotational inertia around the z axis.

$$\begin{aligned} \begin{bmatrix} \dot{\varphi} \\ \dot{\vartheta} \\ \dot{\psi} \end{bmatrix} &= \begin{bmatrix} 1 & sin\,\varphi\,tan\,\vartheta & cos\,\varphi\,tan\,\vartheta \\ 0 & cos\,\varphi & -sin\,\varphi \\ 0 & sin\,\varphi\,sec\,\vartheta & cos\,\varphi\,sec\,\vartheta \end{bmatrix} \begin{bmatrix} p \\ q \\ r \end{bmatrix} \\ &= \begin{bmatrix} \frac{p\,cos\,\vartheta + q\,sin\,\varphi\,sin\,\vartheta + r\,cos\,\varphi\,sin\,\vartheta}{cos\,\vartheta} \\ q\,cos\,\varphi - r\,sin\,\varphi \\ q\,cos\,\varphi - r\,sin\,\varphi \end{bmatrix} \end{aligned} \tag{3}$$

In Eq. (3), $[p\ q\ r]^T$ is the angular velocity and $\dot{\phi}$ $\dot{\theta}$ and $\dot{\psi}$ is the angular velocity, respectively.

According to Eq. (1-3), the model of the conventional quadrotor is

$$\begin{cases} \ddot{x} = \left(C_\varphi C_\psi S_\vartheta + S_\varphi S_\psi\right)\frac{1}{m}u_1 - \frac{k_{dx}}{m}\dot{x} \\ \ddot{y} = \left(C_\varphi S_\vartheta S_\psi - C_\psi S_\varphi\right)\frac{1}{m}u_1 - \frac{k_{dy}}{m}\dot{y} \\ \ddot{z} = C_\vartheta C_\varphi \frac{1}{m}u_1 - \frac{k_{dz}}{m}\dot{z} - g \\ \dot{p} = qr\left(\frac{I_y - I_z}{I_x}\right) + u_2 - \frac{k_{dmx}}{I_x}p + \frac{J_r}{I_x}q(\omega_1 + \omega_3 - \omega_2 - \omega_4) \\ \dot{q} = pr\left(\frac{I_z - I_x}{I_y}\right) + u_3 - \frac{k_{dmy}}{I_y}p + \frac{J_r}{I_y}q(\omega_2 + \omega_4 - \omega_1 - \omega_3) \\ \dot{r} = pq\left(\frac{I_x - I_y}{I_z}\right) + u_4 - \frac{k_{dmz}}{I_z}r \\ \dot{\varphi} = (p\cos\vartheta + q\sin\varphi\sin\vartheta + r\cos\varphi\sin\vartheta)/\cos\vartheta \\ \dot{\vartheta} = q\cos\varphi - r\sin\varphi \\ \dot{\psi} = (q\sin\varphi + r\cos\varphi)/\cos\vartheta \end{cases}. \quad (4)$$

3.2 Dynamic Model of Morphing Quadrotor in Mode Transition Process

The morphing quadrotor has two modes: conventional quadrotor and four-wheeler. The dynamic model of conventional quadrotor is described in Section 3.1. So in this section, the dynamic model of the morphing quadrotor in the mode transition process is analyzed. For simplicity, there are some assumptions:

(1) Four rotor arms maintain simultaneous deformation during mode transition process.

(2) The aerodynamic characteristics of rotors are unchanged.

(3) The attitude angle is not changed during mode transition process.

(4) Friction and other interference between mechanical units are ignored.

(5) Since the four propellers are symmetrical, the torque generated by four rotors can be considered to cancel each other.

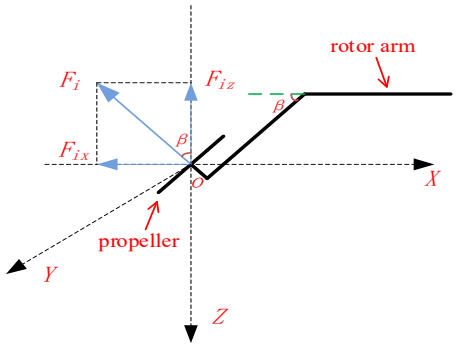

Fig. 3. Force analysis of the morphing quadrotor

Fig. 3 shows one of the rotor arms of the morphing quadrotor.

In the body coordinate system, there is:

$$F_i = \frac{1}{2}\rho A C_i R^2 {\omega_i}^2 = b{\omega_i}^2, \quad i = 1,2,3,4 \tag{5}$$

$$F_{iz} = F_i \cos\beta = \frac{1}{2}\rho A C_i R^2 {\omega_i}^2 \cos\beta = b{\omega_i}^2 \cos\beta. \tag{6}$$

According to the assumption, at this time, the quadrotor is near the ground and only changes in altitude. Hence, four propellers have the same speed. That is, the attitude angle: $\theta = \phi = \psi \approx 0$. Furthermore, there is

$$u_2 = u_3 = u_4 \approx 0\,; u_1 = \sum_1^4 F_{iz}. \tag{7}$$

The original dynamics model becomes:

$$\begin{cases} \ddot{x} = \left(C_\varphi C_\psi S_\vartheta + S_\varphi S_\psi\right)\frac{1}{m}\sum_1^4 F_{iz} - \frac{k_{dx}}{m}\dot{x} \\ \ddot{y} = \left(C_\varphi S_\vartheta S_\psi - C_\psi S_\varphi\right)\frac{1}{m}\sum_1^4 F_{iz} - \frac{k_{dy}}{m}\dot{y}. \\ \ddot{z} = C_\vartheta C_\varphi \frac{1}{m}\sum_1^4 F_{iz} - \frac{k_{dz}}{m}\dot{z} - g \end{cases} \tag{8}$$

4. The Ground Effect of Morphing Quadrotor and the Improvement of the Dynamic Model

All rotorcrafts will be affected by ground effect when landing near the ground. Specially, this is a strong interference to lightweight quadrotor. Ground effect cannot be ignored, otherwise it may cause a devastating disaster [24]. The morphing quadrotor performs deformation when it is near the ground. At this time, not only the lift of the quadrotor changes, but also the ground effect is different as the height drops. Therefore, the situation becomes more complex. In this section, the ground effects of morphing quadrotor will be analyzed and modeled.

4.1 Ground Effect Model of the Morphing Quadrotor

For the morphing quadrotor, the main influencing factors of the ground effect are the height of rotors, the speed and the tilt angle of the rotors. Specially, they are coupled with each other. Therefore, the three factors are analyzed by numerical calculation of flow field.

Firstly, the nonlinear relationship between the height and the tilt angle of the rotor is established, so that they can correspond to each other one by one. Relevant research shows that ground effect is not negligible when the height is four times the rotor diameter. In this paper, the diameter of the rotor is 12.5cm, so the morphing quadrotor starts to deform when it is $0.125\text{m} \times 4 = 0.5\text{m}$ away from the ground and the initial tilt angle of rotor is 0° at this time. When the tilt angle reaches 45°, the height of morphing quadrotor is considered to be 0.3m and the tip of rotor is about to touch the ground at this time. So, there are 200 sets of

correspondence between the height and tilt angle of rotor. Table 1 only shows some of these data to save length of paper.

Table 1

Relationship between the height and the tilt angle of the rotor

Tilt angle /º	height /m	Tilt angle /º	height /m
0	0.500	30	0.400
…	…	…	…
10	0.479	40	0.321
…	…	…	…
20	0.452	45	0.300
…	…	…	…

Then, the centroid height of the quadrotor and the tilt angle of the rotor is taken as the abscissa (unit: m) and as the ordinate (unit: rad), respectively. By the least square curve fitting, their relationship is shown in Fig. 4 and described in Eq. (9).

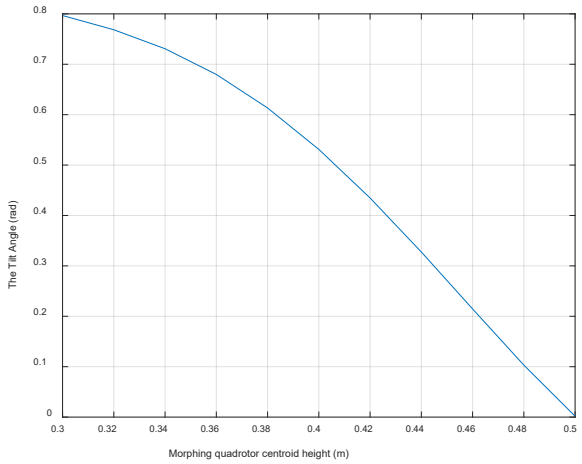

Fig. 4. Fitting curve of the centroid height and the tilt angle

$$\beta = 473.7z^4 - 706.9z^3 + 375.6z^2 - 86.92z + 8.303 \quad (9)$$

In Eq. (9), β is the tilt angle of the rotor, and z is the centroid height of the rotor.

4.2 Fluid Model of Morphing Quadrotor

First, the fluid model of the morphing quadrotor is simplified to four rotors. Different tilt angles and their corresponding heights are modeled in fluid field. The model of the typical tile angle such as 0°and 45°is shown in Fig. 5.

(a) Tilt angle is 0° (b) Tilt angle is 45°

Fig. 5. Fluid model of the morphing quadrotor

By unstructured method, the grid model of Fig. 5 is shown in Fig. 6.

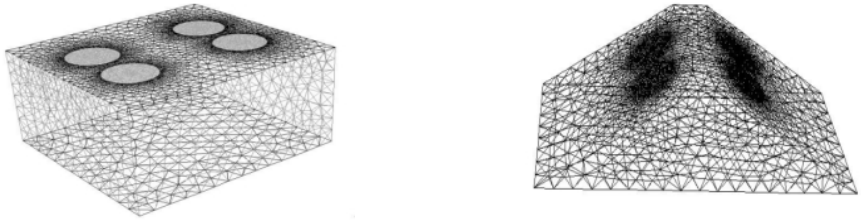

(a) Grid model when the tile angle is 0° (b) Grid model when the tile angle is 45°

Fig. 6. Grid model of the morphing quadrotor in fluid field

The boundary conditions are shown in Fig. 7. The faces around the morphing quadrotor are set to pressure outlet and the ground is set to wall. The speed inlet is the four rotors.

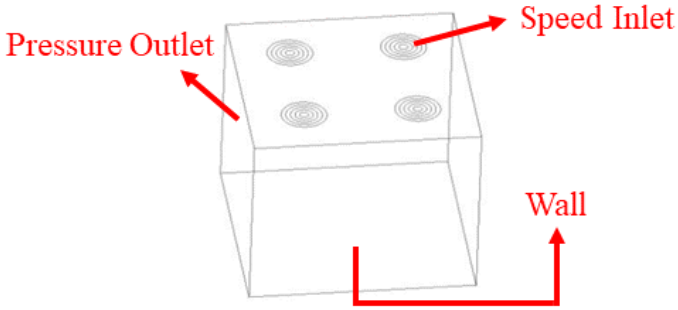

Fig. 7. Setting of Boundary condition in fluid field

4.3 Simulation and Analysis of Ground Effect

According to Table 1 and different velocity of inlet, the ground effect can be simulated by fluid calculations. Fig. 8 shows the simulation result when the tilt angle is 0° and 45°.

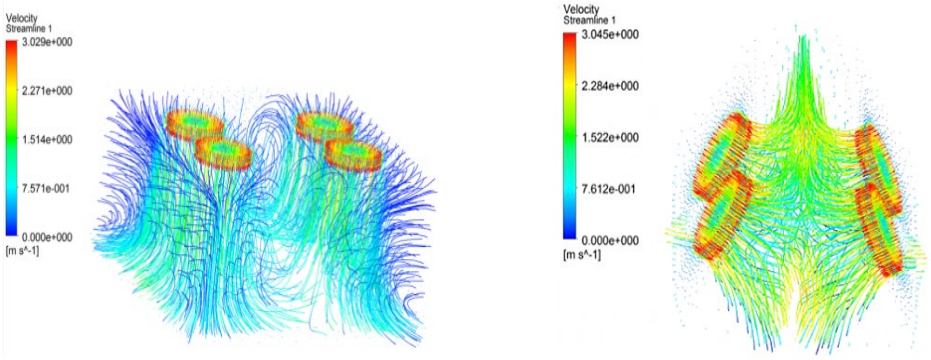

(a) Simulation when tilt angle is 0° (b) Simulation when tilt angle is 45°

Fig. 8. Setting of Boundary condition in fluid field

200 simulations were carried out and part of data is shown in Table 2.

Table 2

Forces of the ground effect corresponding to different heights and velocity of the rotor in mode transition process

Height of rotor \ Velocity of rotor (rad/s) / Force of ground effect/N	100	200	300	400	500
0.50	0.0037	0.035	0.091	0.179	0.360
…	…	…	…	…	…
0.45	0.0035	0.033	0.090	0.176	0.357
…	…	…	…	…	…
0.40	0.0034	0.031	0.088	0.172	0.350
…	…	…	…	…	…
0.35	0.0029	0.026	0.073	0.142	0.284
…	…	…	…	…	…
0.30	0.0025	0.023	0.064	0.125	0.251

Table 2 shows that if the tile angle of the rotor is constant, the influence of the ground effect increases as the velocity of rotor increases. It is consistent with the results of the ground effect in conventional quadrotor. If the velocity of the rotor is constant, the influence of the ground effect decreases as the tile angle of

rotor increases and the height of rotor decreases. It is different from conventional quadrotor. The reason is that the morphing quadrotor losses part of lift when the tilt angle increases during mode transition process.

4.4 Improvement of the Morphing Quadrotor Model with Ground Effect

Basing on the analysis of Section 4.3, in this section, the force of the ground effect will be taken as a part of lift to improve the model of the morphing quadrotor. According to the aerodynamic of the rotors, the lift of the rotor is proportional to the square of its velocity. Near the ground, the ground effect is also related to the velocity of the rotor. Therefore, it is important to find the relationship between the ground effect and velocity of rotor. In order to decouple the height and the ground effect, each data of Table 2 are used in specific height. That is, by changing the velocity of the rotor at each altitude, the relationship between the ground effect and the velocity of the rotor will be obtained. Specially, the velocity of the rotor is from 100 to 500 rad/s. After data fitting, there is

$$\begin{cases} f_{001} = 0.0007\omega - 0.0451, & z = 0.50m \\ \vdots & \vdots \\ f_{100} = 0.0007\omega - 0.0479, & z = 0.40m. \\ \vdots & \vdots \\ f_{200} = 0.0005\omega - 0.0354, & z = 0.30m \end{cases} \tag{10}$$

When the quadrotor is far away from the ground, the rotation of the rotor is controlled by input u_1. According to fluid mechanics, the pressure on the lower surface of the rotor is higher than that on the upper surface, so the quadrotor can fly or hover in the air. When the quadrotor is near the ground, because of the influence of the ground effect, the airflow under the quadrotor is blocked. Then the flow under the quadrotor slows down and a high pressure state is formed, which increases the pressure on the lower surface of the rotor. Therefore, it increases the lift of the quadrotor, and the force of the ground effect is similar to that controlled by u_1. By Eq. (10), the model of the morphing quadrotor in Section 3.3 can be improved as follow.

$$\begin{cases} \ddot{z} = C_\vartheta C_\varphi \frac{1}{m}(u_1 \cos\beta + f_{001}) - \frac{k_{dz}}{m}\dot{z} - g \quad (0.499 < \mathrm{z} \le 0.500)\mathrm{m} \\ \vdots \qquad\qquad \vdots \\ \ddot{z} = C_\vartheta C_\varphi \frac{1}{m}(u_1 \cos\beta + f_{100}) - \frac{k_{dz}}{m}\dot{z} - g \quad (0.399 < \mathrm{z} \le 0.400)\mathrm{m} \\ \vdots \qquad\qquad \vdots \\ \ddot{z} = C_\vartheta C_\varphi \frac{1}{m}(u_1 \cos\beta + f_{200}) - \frac{k_{dz}}{m}\dot{z} - g \quad (0.300 < \mathrm{z} \le 0.301)\mathrm{m} \end{cases} \tag{11}$$

In addition, the attitude angle is assumed to be constant as 0, so the morphing quadrotor can maintain symmetry, and the influence of the ground effect on attitude is no longer considered in the following analysis.

5. Control of Morphing Quadrotor

At present, there are many researches on the control of quadrotor, including classic PID control, backstepping control, neural network adaptive control, adaptive sliding mode control, H_∞ control, LQR control and so on. However, in most of researches, ground effect is usually regarded as interference which does not have model, so some anti-interference controllers such as robust control are preferred. But, these controllers are often conservative. PID control is widely used because of its simple structure and easy operation. On the other hand, LQR control has a good performance on robust and dynamic. So PID and LQR are respectively used to control the mode transition process of the morphing quadrotor and compared with each other.

The overall structure of control system is shown in Fig. 9.

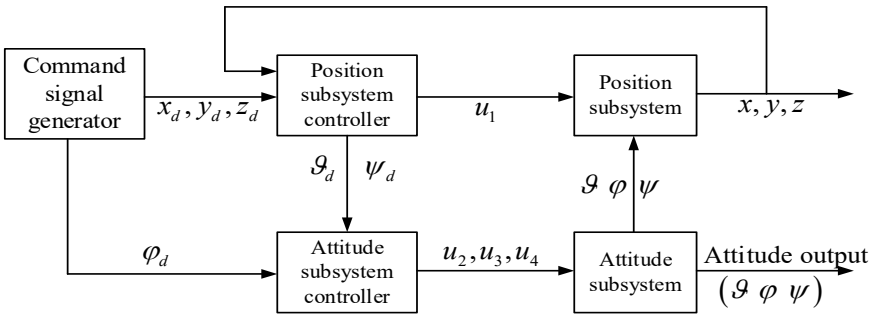

Fig. 9. Control system of morphing quadrotor

The control system is composed of inner and outer loop. The inner and outer loop is responsible for the control of the attitude and position, respectively. The outer loop generates two command signals ψ_d and θ_d, which are transmitted to the inner loop. The inner loop tracks the ψ_d and θ_d by the proper control law.

5.1 Control Law of Attitude Loop

From the analysis in Section 4.4, if the attitude angle does not change or changes little during mode transition process, the influence of ground effect can be ignored. Therefore, the control law of attitude loop is similar to conventional quadrotor. The attitude loop uses PD control because of its better adaptability.

According to the dynamic model of the conventional quadrotor, a reasonable simplification of Eq. (4) is Eq. (12), when the attitude angle changes a little.

$$\begin{cases} \ddot{x} = \left(C_\varphi C_\psi S_\vartheta + S_\varphi S_\psi\right)\frac{1}{m}u_1 - \frac{k_{dx}}{m}\dot{x} \\ \ddot{y} = \left(C_\varphi S_\vartheta S_\psi - C_\psi S_\varphi\right)\frac{1}{m}u_1 - \frac{k_{dy}}{m}\dot{y} \\ \ddot{z} = C_\vartheta C_\varphi \frac{1}{m}u_1 - g - \frac{k_{dz}}{m}\dot{z} \\ \ddot{\vartheta} = u_2 - \frac{lk_{dmx}}{I_x}\dot{\vartheta} \\ \ddot{\varphi} = u_3 - \frac{lk_{dmy}}{I_y}\dot{\varphi} \\ \ddot{\psi} = u_4 - \frac{lk_{dmz}}{I_z}\dot{\psi} \end{cases} \tag{12}$$

The target of PD control is to realize $\theta \to \theta_d$, $\phi \to \phi_d$ and $\psi \to \psi_d$. Let $\theta_e = \theta - \theta_d$ and use PD control method based on feedforward compensation, so the control law is:

$$u_2 = -k_{p4}\vartheta_e - k_{d4}\dot{\vartheta}_e + \ddot{\vartheta}_d + \frac{lk_{dmx}}{I_x}\dot{\vartheta}_d. \tag{13}$$

Then, $\ddot{\vartheta} = -k_{p4}\vartheta_e - k_{d4}\dot{\vartheta}_e + \ddot{\vartheta}_d - \frac{lk_{dmx}}{I_x}\dot{\vartheta}_e$ and $\ddot{\vartheta}_e + \left(k_{d4} + \frac{lk_{dmx}}{I_x}\right)\dot{\vartheta}_e + k_{p4}\vartheta_e = 0$. According to the Hurwitz criterion of the second-order system, there should be $k_{p4} > 0$ and $k_{d4} + \frac{lk_{dmx}}{I_x} > 0$. So $k_{p4} = k_{d4} = 15.0$.

Similarly u_3 and u_4 are given by:

$$\begin{cases} u_3 = -k_{p5}\varphi_e - k_{d5}\dot{\varphi}_e + \ddot{\varphi}_d + \frac{lk_{dmy}}{I_y}\dot{\varphi}_d \\ u_4 = -k_{p6}\psi_e - k_{d6}\dot{\psi}_e + \ddot{\psi} + \frac{lk_{dmz}}{I_z}\dot{\psi}_d \end{cases}, \tag{14}$$

where $k_{p5} = k_{d5} = 15.0$ and $k_{p6} = k_{d6} = 15.0$.

5.2 Control Law of Height Loop

In Section 3.2, it is assumed that the four rotor arms maintain symmetrical during mode transition process. So the torque generated by four propellers cancels each other and it is assumed that the morphing quadrotor will not move in the horizontal direction. Therefore, the position loop focuses on the altitude control and it can be simplified to a height loop.

5.2.1 Height Controller Based on PID

Regarding to the height loop, there is a significant difference between the mode transition state (with ground effect) and the conventional quadrotor state

(without ground effect). So, the height controller with ground effect is designed as follows.

First, by the control of u_1, the system hopes to realize $x \to 0, y \to 0$ and $z \to z_d$. According to Eq. (3-8), define:

$$u_{1x} = u_1(C_\varphi C_\psi S_\vartheta + S_\varphi S_\psi)/m \tag{15}$$

$$u_{1y} = u_1(C_\varphi S_\vartheta S_\psi - C_\psi S_\varphi)/m \tag{16}$$

$$u_{1z} = C_\vartheta C_\varphi(u_1 \cos\beta + f)/m \tag{17}$$

Then, the model of the position is

$$\ddot{x} = u_{1x} - \frac{k_{dx}}{m}\dot{x} \tag{18}$$

$$\ddot{y} = u_{1y} - \frac{k_{dy}}{m}\dot{y} \tag{19}$$

$$\ddot{z} = u_{1z} - g - \frac{k_{dz}}{m}\dot{z} \tag{20}$$

So the height controller based on PD method is

$$u_{1z} = -k_{pz}z_e - k_{dz}\dot{z}_e + g + \ddot{z}_d + \frac{1}{m}(k_3\dot{z}_d + f). \tag{21}$$

Furthermore, $\ddot{z}_e + \left(k_{dz} + \frac{k_3}{m}\right)\dot{z}_e + k_{pz}z_e + \frac{f}{m} = 0$. According to the Hurwitz criterion of the second-order system, the stability condition of $as^2 + a_1 s + a_0 = 0$ is

$$\begin{cases} a_0, a_1, a_2 > 0 \\ a_1 a_0 > 0 \end{cases}. \tag{22}$$

Thus, the proper parameters should be found to make $k_{pz} > 0$ and $k_{dz} + k_3/m > 0$. Here, $k_{pz} = k_{dz} = 55.0$.

Similarly, $\begin{cases} u_{1x} = -k_{px}x - k_{dx}\dot{x} \\ u_{1y} = -k_{py}y - k_{dy}\dot{y} \end{cases} \Rightarrow \begin{cases} k_{px} = k_{dx} = 35.0 \\ k_{py} = k_{dy} = 35.0 \end{cases}$.

5.2.2 Height Controller Based on LQR

In order to ensure the feasibility, the paper designs another height controller based on LQR method. The control system is as follows.

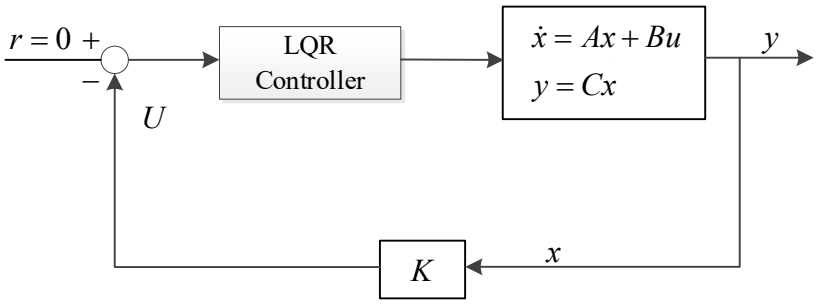

Fig. 10. Height controller based on LQR

Since many researches have introduced LQR method [25], the section focuses on the control cost and the objective function can be written as:

$$J = \frac{1}{2}\int_0^{\infty}[x^T(t)Qx(t) + u^T(t)Ru(t)]dt. \quad (23)$$

First, the parameters R and Q of the LQR optimal controller are selected. Here, the weighting matrix Q is $Q = \mathrm{diag}(q_{11}\ q_{22}\ )$ and the coefficients q_{11} and q_{22} have a great influence on the performance of the control system. By adjusting the coefficients q_{11} and q_{22}, the LQR controller can be uesed according to different demands. In the actual design, an optimal balance point should be found between the output and the input.

Through lots of experiments, it is more appropriate to use $R = \mathrm{diag}(1)$ and $Q = \mathrm{diag}(100\ 1)$. According to Eq. (23) and parameters (which is shown in Table 3 of Section 6.1), there is $A = [0\ 1; 0\ -0.05]$ and $B = [0; 1]$. The feedback gain of the state feedback equation is $K = [10 \quad 4.5776]$.

6. Simulation and Analysis

6.1 Parameters of Simulation

The simulation parameters of the morphing quadrotor are shown in Table 3.

Table 3

Simulation parameters of the morphing quadrotor

Parameter	Value	Unit
Body mass (m)	2	kg
Acceleration of gravity (g)	9.8	m/s^2
Distance from rotor center to body center of mass (l)	0.2	m
Lift coefficient (b)	3.5×10^{-5}	
Translational resistance coefficient (k_d)	diag(0.01 0.01 0.01)	
Rotational resistance torque coefficient (k_{dm})	diag(0.012 0.012 0.012)	
Triaxial inertia (I)	diag(1.25 1.25 2.5)	kg/m^2

According to the analysis in Section 5, the control system of the morphing quadrotor is shown in Fig. 11.

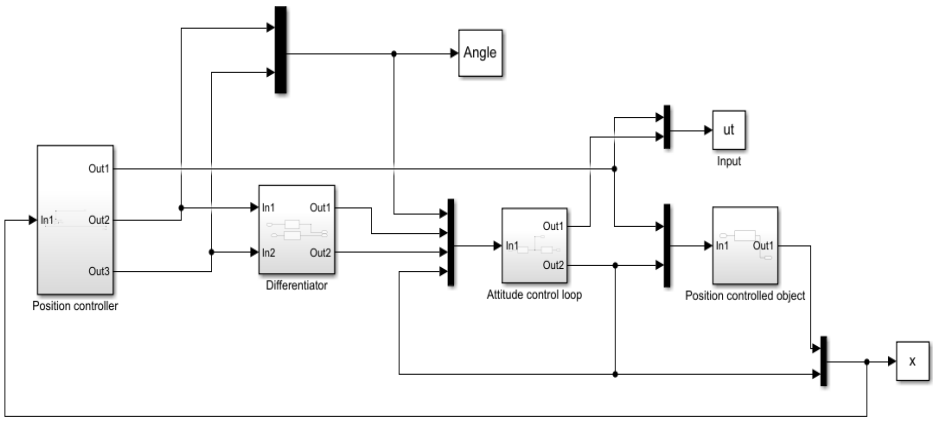

Fig. 11. Control system of the morphing quadrotor in simulation environment

Here, the convergence speed of the inner loop should be greater than that of the outer loop, which ensures the stability of whole system. Therefore, the gain of the inner loop controller is greater than that of the outer loop controller.

6.2 Simulation of the mode transition process with ground effect

Initial state of position is $[x\ \dot{x}\ y\ \dot{y}\ z\ \dot{z}] = [0\ 0\ 0\ 0\ 0.6\ 0]$.
Initial state of attitude angle is $[\vartheta\ \dot{\vartheta}\ \varphi\ \dot{\varphi}\ \psi\ \dot{\psi}] = [0\ 0\ 0\ 0\ 0\ 0]$.
Desired position is $[x_d\ y_d\ z_d] = [0\ 0\ 0.3]$.
Desired attitude angle is $[\vartheta_d\ \varphi_d\ \psi_d] = [0\ 0\ 0]$.

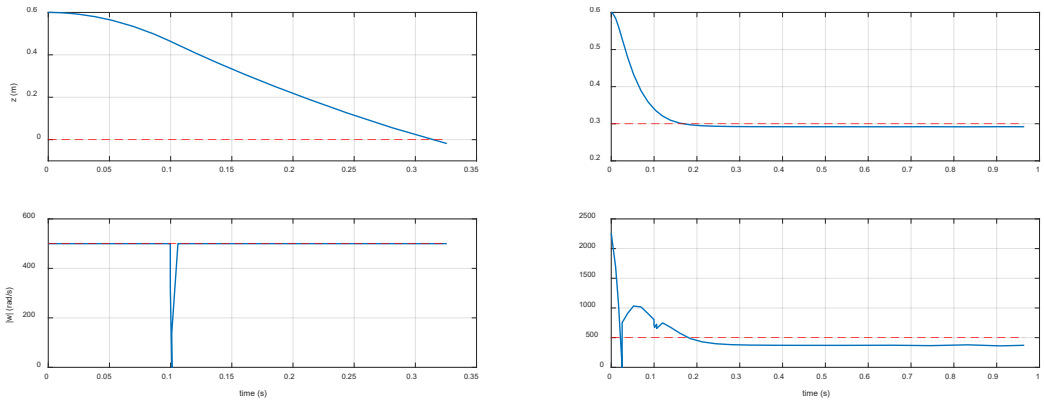

(a) The maximum rotor speed is 500rad/s (b) The maximum rotor speed is infinite

Fig. 12. Performance of altitude and rotor speed by PD control

Fig. 12 shows the simulation results of autonomous landing control under the PD control; as described in section 4.1, the maximum rotor speed is 500rad/s. Due to the excessive loss of lift during the landing, even if the maximum speed is maintained continuously, the ground collision situation still occurs at 0.3s (Fig. 12(a)). If the speed is not limited, it only takes 0.2s to stabilize the quad-rotor at 0.15m (Fig. 12(b)), indicating that if the morphing quadrotor wants to achieve autonomous landing, it is recommended to add the lift compensation to keep the deformation stable.

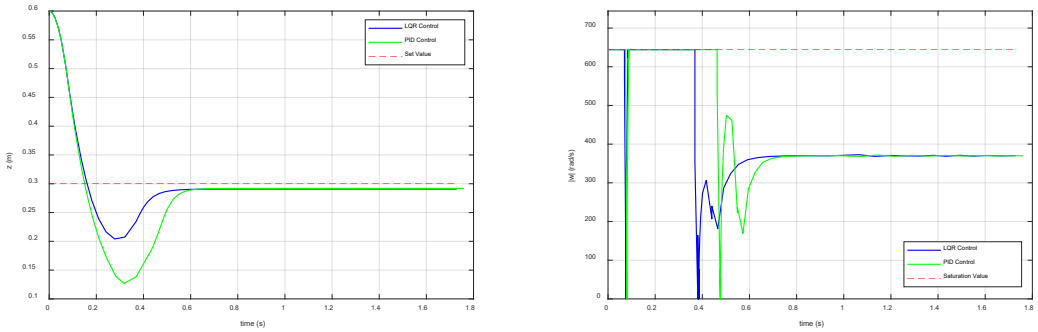

Fig. 13. Autonomous landing control with maximum rotor speed increased to 644rad/s

According to the changes of the height Z in Fig. 13, the landing process of LQR is smoother than that of PID. Specially, there is a huge overshoot in the height control of PID. This situation may lead to a disaster, even if the steady-state error value of PID is smaller. Therefore, the height control of LQR is better than that of PID.

The Fig. 13 also shows that in the case of limited control input, regardless of whether LQR control or PID control is used, the additional compensation of the lift is required to make the deformation process stable. It is recommended to add the lift compensation to achieve a smooth transition.

7. Conclusion

The paper proposes a novel morphing quadrotor which can be transformed into a four-wheeler when landing. Then, the ground effect of the mode transition process is analyzed by fluid calculation. Furthermore, the model of the morphing quadrotor with ground effect is proposed. Basing on PID and LQR, the control system of the morphing quadrotor is designed and compared. By the simulation and analysis, the main conclusions are as follows:

(1) The ground effect of the morphing quadrotor is more complex than that of conventional quadrotor. When the velocity of the rotor is constant, the ground effect gradually decreases as the height decreases and the tilt angle of the rotor

increases. It is because after the rotor tilts, the vertical component of the rotor force loses much.

(2) When the rotation speed of the rotor is limited, it is necessary to compensate for the lift with additional input, so that the autonomous landing will keep stable..

(3) Compared with PID, LQR control has a smoother mode transition process.

In the future, we will consider how to compensate for the extra lift required during autonomous landing of the morphing quadrotor from various perspectives. And how to realize the optimization and self-tuning of the LQR control parameters during the landing process are also the key contents in our future work.

Acknowledgement

This work was supported in part by National Natural Science Foundation of China under Grant 61973222 and 61503255, Natural Science Foundation of Liaoning Province under Grant 2019-ZD-0247 and Fundamental Research Funds for the Universities of Liaoning Province.

REFERENCES

[1]. *J. Ni, G. Tang, Z. Mo, W. Cao and S. X. Yang*,"An Improved Potential Game Theory Based Method for Multi-UAV Cooperative Search", in IEEE Access, **vol. 8**, 2020, pp. 47787-47796

[2]. *M. Atif, R. Ahmad, W. Ahmad, L. Zhao and J. J. P. C. Rodrigues*,"UAV-Assisted Wireless Localization for Search and Rescue", in IEEE Systems Journal, **vol. 15**, no. 3, Sept. 2021, pp. 3261-3272

[3]. *C. Zhang, P. M. Atkinson, C. George, Z. Wen, M. Diazgranados and F. Gerard*,"Identifying and mapping individual plants in a highly diverse high-elevation ecosystem using UAV imagery and deep learning", in ISPRS Journal of Photogrammetry and Remote Sensing, **vol. 169**, 2020, pp. 280-291

[4]. *Y. Zeng, J. Xu and R. Zhang*,"Energy Minimization for Wireless Communication With Rotary-Wing UAV", in IEEE Transactions on Wireless Communications, **vol. 18**, no. 4, April 2019, pp. 2329-2345

[5]. *V. Riviere, A. Manecy and S. Viollet*,"Agile robotic fliers: A morphing-based approach", in Soft robotics, **vol. 5**, no. 5, 2018, pp. 541-553

[6]. *M. Kamel, S. Verling, O. Elkhatib, C. Sprecher, P. Wulkop, Z. Taylor, R. Siegwart and I. Gilitschenski*,"The Voliro omniorientational hexacopter: An agile and maneuverable tiltable-rotor aerial vehicle", in IEEE Robotics & Automation Magazine, **vol. 25**, no. 4, Dec. 2018, pp. 34-44

[7]. *A. Desbiez, F. Expert, M. Boyron, J. Diperi, S. Viollet and F. Ruffier*,"X-Morf: A crash-separable quadrotor that morfs its X-geometry in flight", Workshop on Research, Education and Development of Unmanned Aerial Systems (RED-UAS), Linköping, Sweden, 2017, pp. 222-227

[8]. *M. Zhao, K. Kawasaki, X. Chen, S. Noda, K. Okada and M. Inaba*,"Whole-body aerial manipulation by transformable multirotor with two-dimensional multilinks", IEEE International Conference on Robotics and Automation (ICRA), Singapore, 2017, pp. 5175-5182

[9]. *M. Zhao, T. Anzai, F. Shi, X. Chen, K. Okada and M. Inaba*,"Design, Modeling, and Control of an Aerial Robot DRAGON: A Dual-Rotor-Embedded Multilink Robot With the Ability of Multi-Degree-of-Freedom Aerial Transformation", in IEEE Robotics and Automation Letters, **vol. 3**, no. 2, April 2018, pp. 1176-1183

[10]. *L. Daler, A. Klaptocz, A. Briod, M. Sitti and D. Floreano*,"A perching mechanism for flying robots using a fibre-based adhesive", IEEE International Conference on Robotics and Automation, Karlsruhe, Germany, 2013, pp. 4433-4438

[11]. *J. Moore and R. Tedrake*,"Magnetic localization for perching UAVs on powerlines", IEEE/RSJ International Conference on Intelligent Robots and Systems, San Francisco, CA, USA, 2011, pp. 2700-2707

[12]. *M. Keennon, K. Klingebiel and H. Won*,"Development of the Nano Hummingbird: A Tailless Flapping Wing Micro Air Vehicle", 50th AIAA aerospace sciences meeting including the new horizons forum and aerospace exposition, Nashville, TN, USA, 2012, pp. 588

[13]. *D. Floreano and R. J. Wood*,"Science, technology and the future of small autonomous drones", in Nature, **vol. 521**, 2015, pp. 460-466

[14]. *W. Zhao, H. Liu and F. L. Lewis*,"Robust Formation Control for Cooperative Underactuated Quadrotors via Reinforcement Learning", in IEEE Transactions on Neural Networks and Learning Systems, **vol. 32**, no. 10, Oct. 2021, pp. 4577-4587

[15]. *H. E. Glida, L. Abdou, A. Chelihi, C. Sentouh and S. Hasseni*,"Optimal model-free backstepping control for a quadrotor helicopter", in Nonlinear Dynamics, **vol. 100**, 2020, pp. 3449-3468

[16]. *S. C. Yogi, V. K. Tripathi and L. Behera*,"Adaptive Integral Sliding Mode Control Using Fully Connected Recurrent Neural Network for Position and Attitude Control of Quadrotor", in IEEE Transactions on Neural Networks and Learning Systems, **vol. 32**, no. 12, Dec. 2021, pp. 5595-5609

[17]. *R. B. Anderson, J. A. Marshall and A. L'Afflitto*,"Constrained Robust Model Reference Adaptive Control of a Tilt-Rotor Quadcopter Pulling an Unmodeled Cart", in IEEE Transactions on Aerospace and Electronic Systems, **vol. 57**, no. 1, Feb. 2021, pp. 39-54

[18]. *A. Noormohammadi-Asl, O. Esrafilian, M. A. Arzati and H. D. Taghirad*,"System identification and H∞ -based control of quadrotor attitude", in Mechanical Systems and Signal Processing, **vol. 135**, 2020, 106358

[19]. *R. Miranda-Colorado and L. T. Aguilar*,"Robust PID control of quadrotors with power reduction analysis", in ISA transactions, **vol. 98**, 2020, pp. 47-62

[20]. *P. E. Tanner, A. D. Overmeyer, L. N. Jenkins, C. Yao and S. M. Bartram*,"Experimental investigation of rotorcraft outwash in ground effect", AHS International Annual Forum & Technology Display, Virginia Beach, VA, USA, 2015

[21]. *Z. Trivković, J. Svorcan, M. Baltić, D. Komarov and V. Fotev*,"Computational analysis of helicopter main rotor blades in ground effect", in Scientific Technical Review, **vol. 66**, no. 4, 2016, pp. 52-58

[22]. *B. M. Kutz, M. Keßler and E. Krämer*,"Experimental and numerical examination of a helicopter hovering in ground effect", in CEAS Aeronautical Journal, **vol. 4**, 2013, pp. 397–408

[23]. *Y. Wang, J. Sun, H. He and C. Sun*,"Deterministic Policy Gradient With Integral Compensator for Robust Quadrotor Control", in IEEE Transactions on Systems, **vol. 50**, no. 10, Oct. 2020, pp. 3713-3725

[24]. *X. Liang, G. Meng, X. Chen and T. Zhang*,"A Novel Model Reference Adaptive Controller of Quad-Rotor on Autonomous Take-off and Landing with Ground Effect", in International Journal of Simulation Systems. Science & Technology, **vol. 17**, no. 24, 2016, pp. 31

[25]. *A. Alaimo, V. Artale, G. Barbaraci, C. L. R. Milazzo, C. Orlando and A. Ricciardello*,"LQR-PID control applied to hexacopter flight", in Journal of Numerical Analysis, Industrial and Applied Mathematics, **vol. 9**, no. 3-4, 2016, pp. 47-56